*Supporting information*

# Antibacterial Activity of Two Zn-MOFs Containing a Tricarboxylate Linker

**Sara Rojas [1], Amalia García-García [1], Tania Hidalgo [2], María Rosales [1], Daniel Ruiz-Camino [2], Pablo Salcedo-Abraira [2], Helena Montes-Andrés [1], Duane Choquesillo-Lazarte [3], Roberto Rosal [4], Patricia Horcajada [2,*] and Antonio Rodríguez-Diéguez [1,*]**

[1] Department of Inorganic Chemistry, Faculty of Science, University of Granada, Av. Fuentenueva s/n, 18071 Granada, Spain
[2] Advanced Porous Materials Unit, IMDEA Energy Institute, Av. Ramón de la Sagra 3, 28935 Móstoles, Spain
[3] Laboratorio de Estudios Cristalográficos, IACT-CSIC, Av. de las Palmeras, 4, 18100 Armilla, Spain
[4] Department of Chemical Engineering, University of Alcalá, 28871 Alcalá de Henares, Spain
* Correspondence: patricia.horcajada@imdea.org (P.H.); antonio5@ugr.es (A.R.-D.)

**Table of content**



## S1. Coordination modes

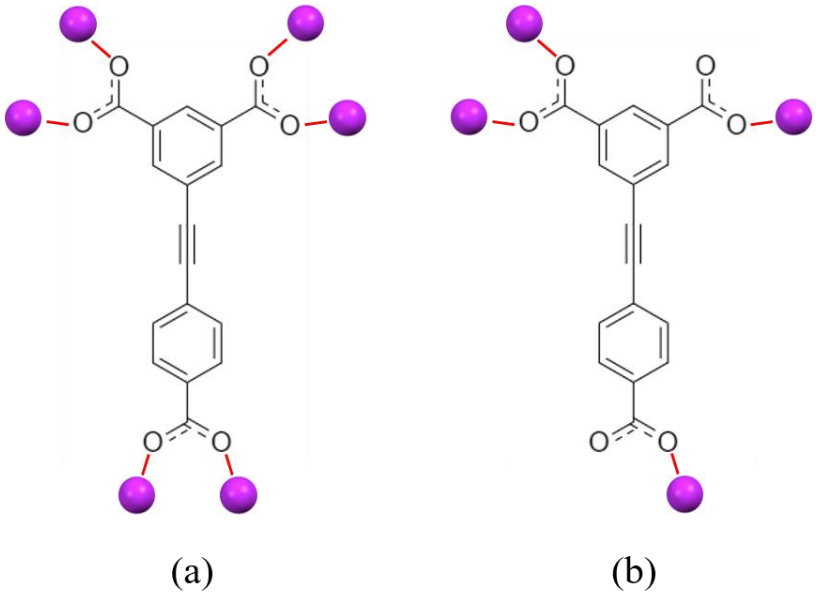


**Figure S1.** Coordination modes of the linker $H_3L$ in the new MOFs. GR-MOF-8 contains modes (a) and (b), whereas GR-MOF-9 is made of linkers with coordination mode (a). Metal ions are indicated in purple color.

## S2. Crystallographic information

**Table S1.** Table of the selected bond lengths (Å) and angles (°) for GR-MOF-8.

| Bond | Distance (Å) | Angle | Degree (°) |
|---|---|---|---|
| Zn1-O1 | 1.985(10) | O1-Zn1-O22 | 104.6(5) |
| Zn1-O22 | 1.995(11) | O1-Zn1-O24 | 111.7(4) |
| Zn1-O24 | 1.931(9) | O1-Zn1-O25 | 102.7(6) |
| Zn1-O25 | 1.947(14) | O22-Zn1-O24 | 110.7(4) |
| Zn2-O8 | 1.967(9) | O22-Zn1-O25 | 114.2(5) |
| Zn2-O23 | 2.000(9) | O24-Zn1-O25 | 112.4(5) |
| Zn2-O24 | 1.969(8) | O8-Zn2-O23 | 101.7(4) |
| Zn2-O28 | 1.951(9) | O8-Zn2-O24 | 108.3(3) |
| Zn3-O2 | 1.974(11) | O8-Zn2-O28 | 109.6(4) |
| Zn3-O9 | 1.910(10) | O23-Zn2-O24 | 110.9(4) |
| Zn3-O24 | 1.943(7) | O23-Zn2-O28 | 103.9(4) |
| Zn3-O36 | 1.931(10) | O24-Zn2-O28 | 120.8(4) |
| Zn4-O24 | 1.929(9) | O2-Zn3-O9 | 107.0(5) |
| Zn4-O27 | 2.011(11) | O2-Zn3-O24 | 108.9(4) |
| Zn4-O35 | 2.008(9) | O2-Zn3-O36 | 107.4(5) |
| Zn4-O49 | 1.971(8) | O9-Zn3-O24 | 111.6(4) |
| | | O9-Zn3-O36 | 112.5(4) |
| | | O24-Zn3-O36 | 109.2(4) |
| | | O24-Zn4-O27 | 108.6(5) |
| | | O24-Zn4-O35 | 112.3(4) |
| | | O24-Zn4-O49 | 121.9(4) |
| | | O27-Zn4-O35 | 100.9(5) |
| | | O27-Zn4-O49 | 110.2(4) |
| | | O35-Zn4-O49 | 100.8(4) |
| | | Zn1-O24-Zn2 | 108.1(4) |
| | | Zn1-O24-Zn3 | 110.1(4) |
| | | Zn1-O24-Zn4 | 107.7(4) |
| | | Zn2-O24-Zn3 | 108.7(4) |
| | | Zn2-O24-Zn4 | 112.0(4) |
| | | Zn3-O24-Zn4 | 110.2(4) |

**Table S2.** Table of the selected bond lengths (Å) and angles (°) for GR-MOF-9.

| Bond | Distance (Å) | Angle | Degree (°) |
|---|---|---|---|
| Zn00-O005 | 1.97(2) | O005-Zn00-O009 | 100.7(11) |
| Zn00-O009 | 2.14(3) | O005-Zn00-O00B | 100.6(11) |
| Zn00-O00B | 2.13(3) | O005-Zn00-O0AA | 105.8(11) |
| Zn00-O1 | 1.92(7) | O005-Zn00-O1A | 108(2) |
| Zn00-O0AA | 2.00(3) | O009-Zn00-O1A | 151(2) |
| Zn00-O1A | 2.14(6) | O00B-Zn00-O009 | 86.2(11) |
| Zn1-O005 | 1.95(3) | O00B-Zn00-O1A | 91.2(18) |
| Zn1-O00E | 2.04(3) | O1-Zn00-O005 | 104.9(19) |
| Zn1-O00T | 1.96(6) | O1-Zn00-O009 | 153(2) |
| Zn1-O3 | 1.94(3) | O1-Zn00-O00B | 80(2) |
| Zn1-O8CA | 2.33(6) | O1-Zn00-O0AA | 97.0(17) |
| Zn2-O005 | 1.96(3) | O0AA-Zn00-O009 | 84.6(11) |
| Zn2-O00D | 2.05(3) | O0AA-Zn00-O00B | 153.2(11) |
| Zn2-O00J | 1.93(3) | O0AA-Zn00-O1A | 84.9(19) |
| Zn2-O01X | 1.94(6) | O005-Zn1-O00E | 108.5(11) |
| Zn2-O0CA | 2.33(6) | O005-Zn1-O00T | 121(2) |
| Zn04-O005 | 2.00(3) | O005-Zn1-O8CA | 83.6(15) |
| Zn04-O00K | 2.05(6) | O00E-Zn1-O8CA | 153.7(17) |
| Zn04-O2 | 2.07(6) | O00T-Zn1-O00E | 100.7(19) |
| Zn04-O1AA | 2.05(6) | O00T-Zn1-O8CA | 54(2) |
| Zn04-O2AA | 2.04(6) | O3-Zn1-O005 | 113.0(11) |
| Zn04-O3AA | 1.97(3) | O3-Zn1-O00E | 100.7(13) |
| | | O3-Zn1-O00T | 111(2) |
| | | O3-Zn1-O8CA | 95.4(18) |
| | | O005-Zn2-O00D | 108.0(11) |
| | | O005-Zn2-O0CA | 83.5(15) |
| | | O00D-Zn2-O0CA | 155.0(16) |
| | | O00J-Zn2-O005 | 112.7(11) |
| | | O00J-Zn2-O00D | 100.8(13) |
| | | O00J-Zn2-O01X | 112(2) |
| | | O00J-Zn2-O0CA | 94.6(17) |
| | | O01X-Zn2-O005 | 120(2) |
| | | O01X-Zn2-O00D | 101.1(18) |
| | | O01X-Zn2-O0CA | 55(2) |
| | | O005-Zn04-O00K | 94.6(18) |
| | | O005-Zn04-O2 | 94.4(19) |
| | | O005-Zn04-O1AA | 94.5(18) |
| | | O005-Zn04-O2AA | 95(2) |
| | | O1AA-Zn04-O2 | 171(3) |
| | | O2AA-Zn04-O00K | 170(3) |
| | | O3AA-Zn04-O005 | 177.6(12) |

| | | |
|---|---|---|
| | O3AA-Zn04-O00K | 84.4(19) |
| | O3AA-Zn04-O2 | 87.7(19) |
| | O3AA-Zn04-O1AA | 83.6(19) |
| | O3AA-Zn04-O2AA | 86(2) |
| | Zn00-O005-Zn1 | 109.2(12) |
| | Zn00-O005-Zn2 | 108.7(12) |
| | Zn00-O005-Zn04 | 107.9(11) |
| | Zn1-O005-Zn2 | 110.8(11) |
| | Zn1-O005-Zn04 | 110.3(12) |
| | Zn2-O005-Zn04 | 109.9(12) |

**S3. Physicochemical characterization**

The lattice parameters were refined using TOPAS software (version 5, Bruker AXS, Karlsruhe, Germany). There is a good agreement between the data and the model.

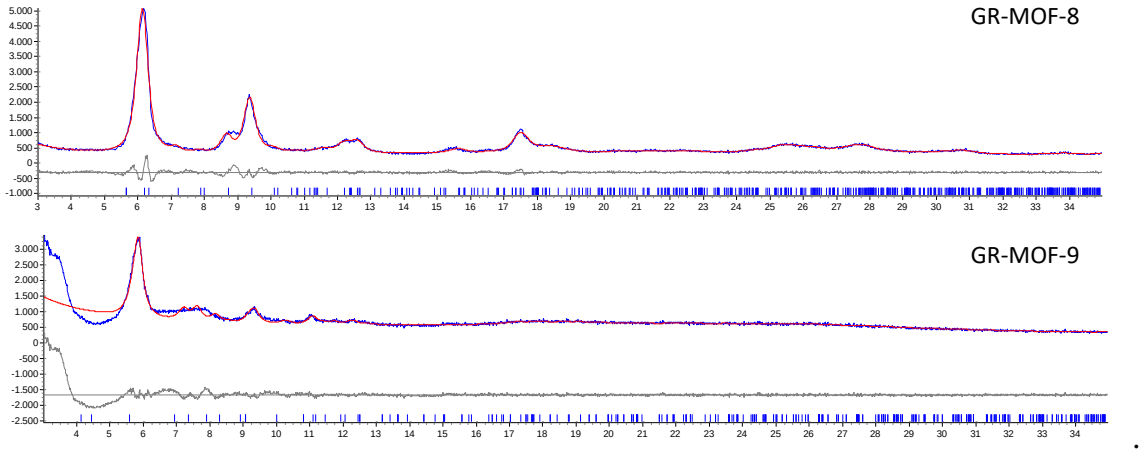


**Figure S2.** Le Bail fitting of GR-MOF-8 and 9.

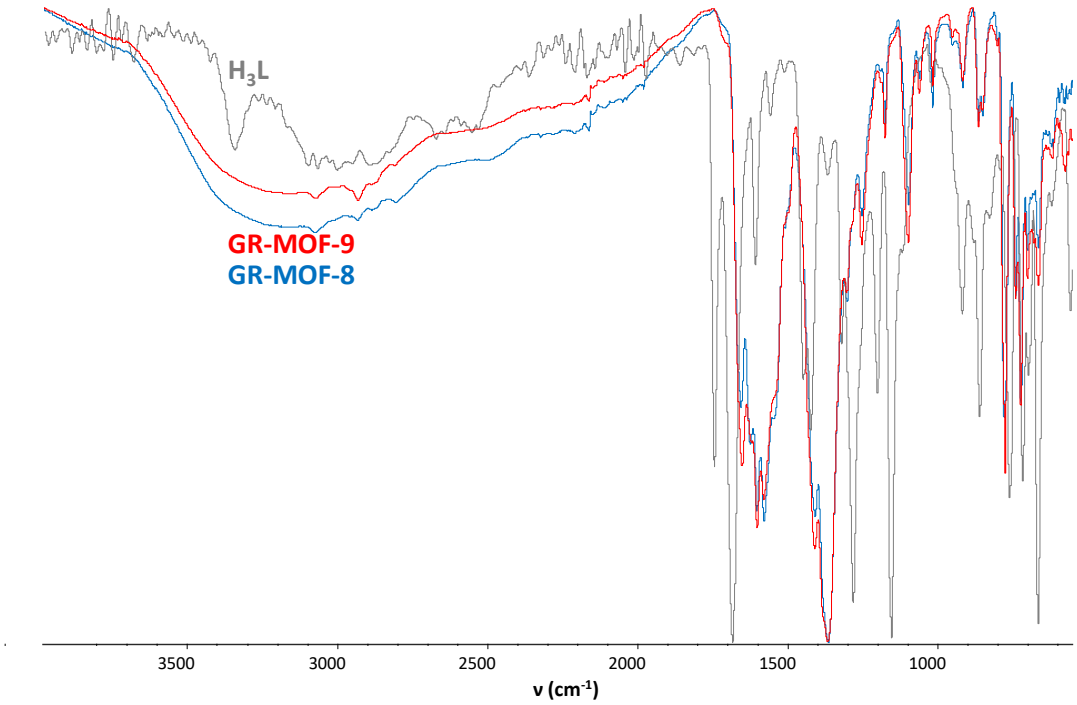


**Figure S3.** Fourier transform infrared spectroscopy (FTIR) spectra of the GR-MOF-8 (blue) and 9 (red), and the $H_3L$ linker (grey).

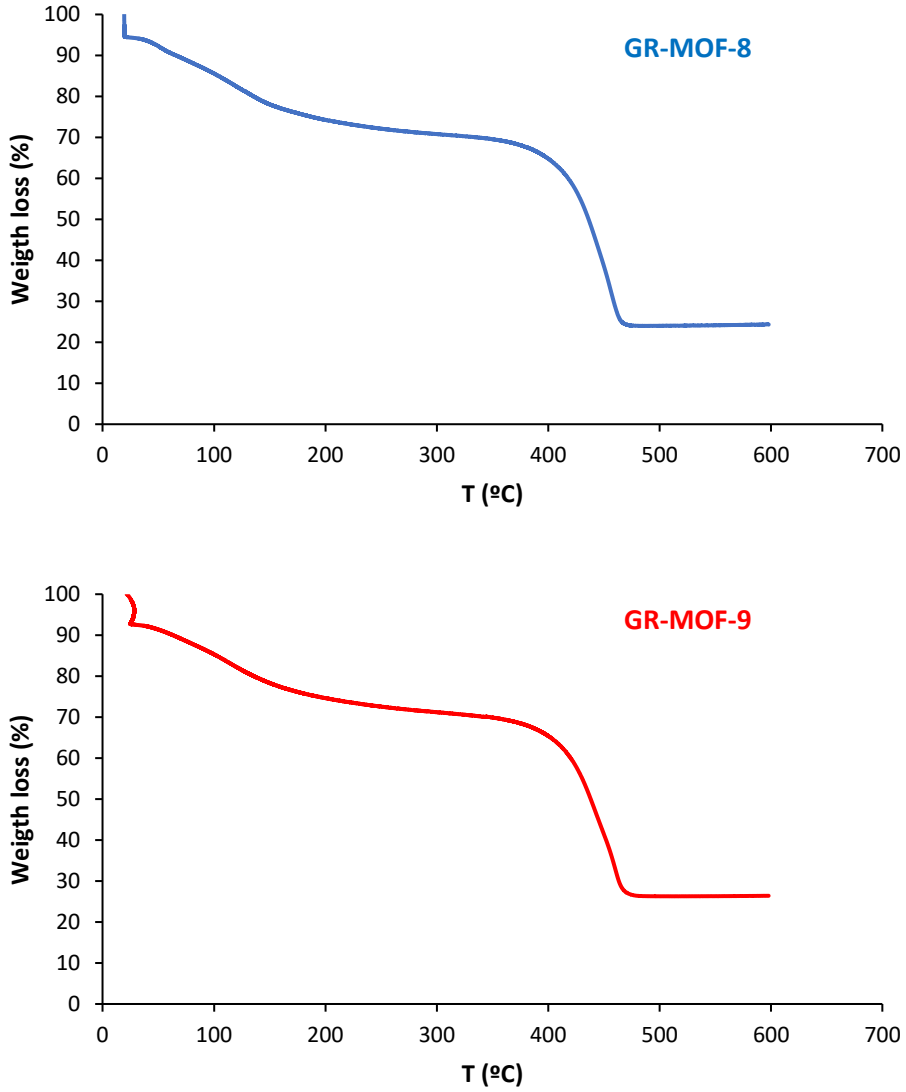


**Figure S4.** Thermogravimetric analysis (TGA) of the GR-MOF-8 and 9 materials.

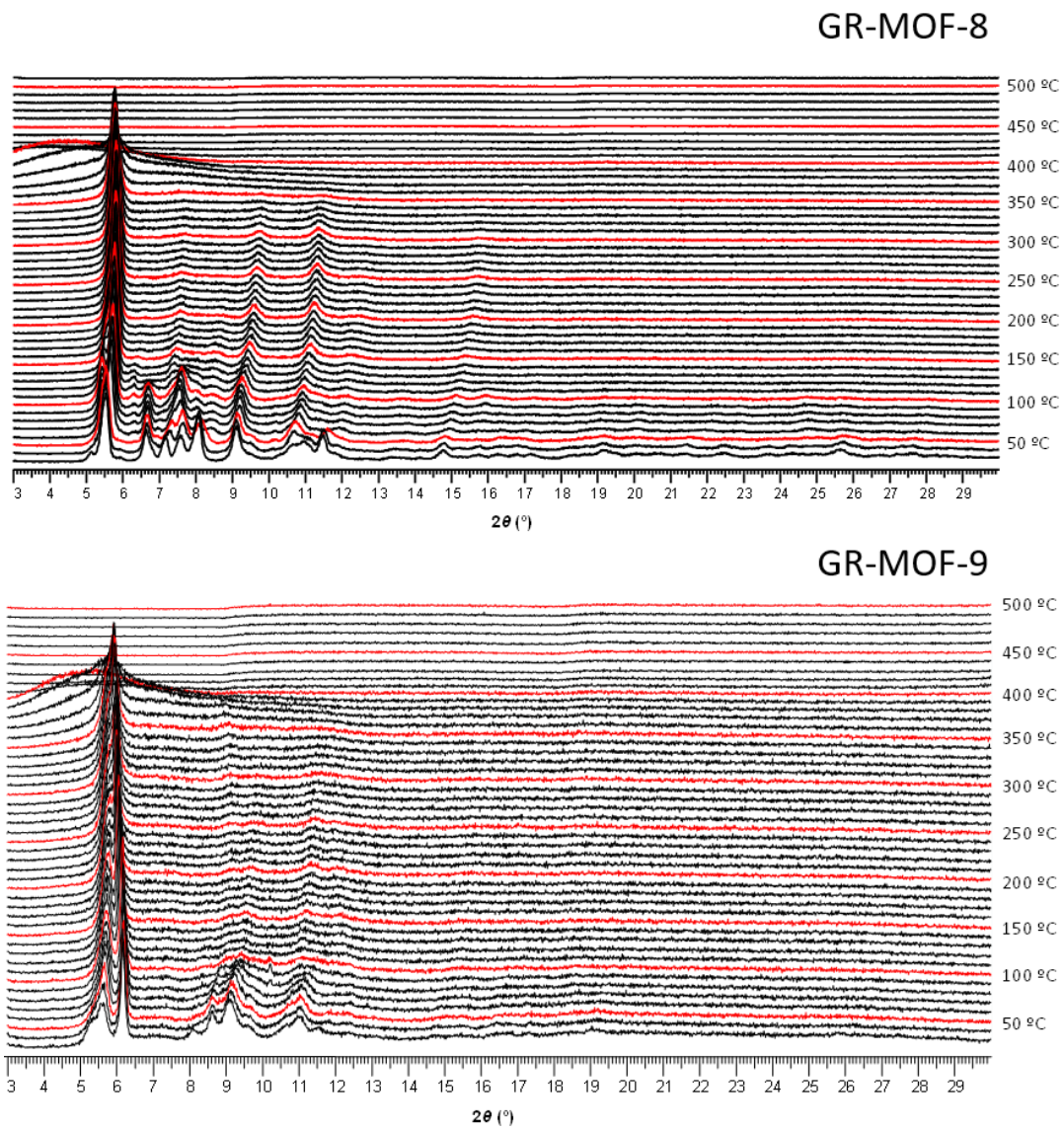


**Figure S5.** Variable-temperature powder X-ray diffraction (VTPXRD) of the GR-MOF-8 and 9 materials from 25 to 500 °C.

## S4. Antibacterial activity

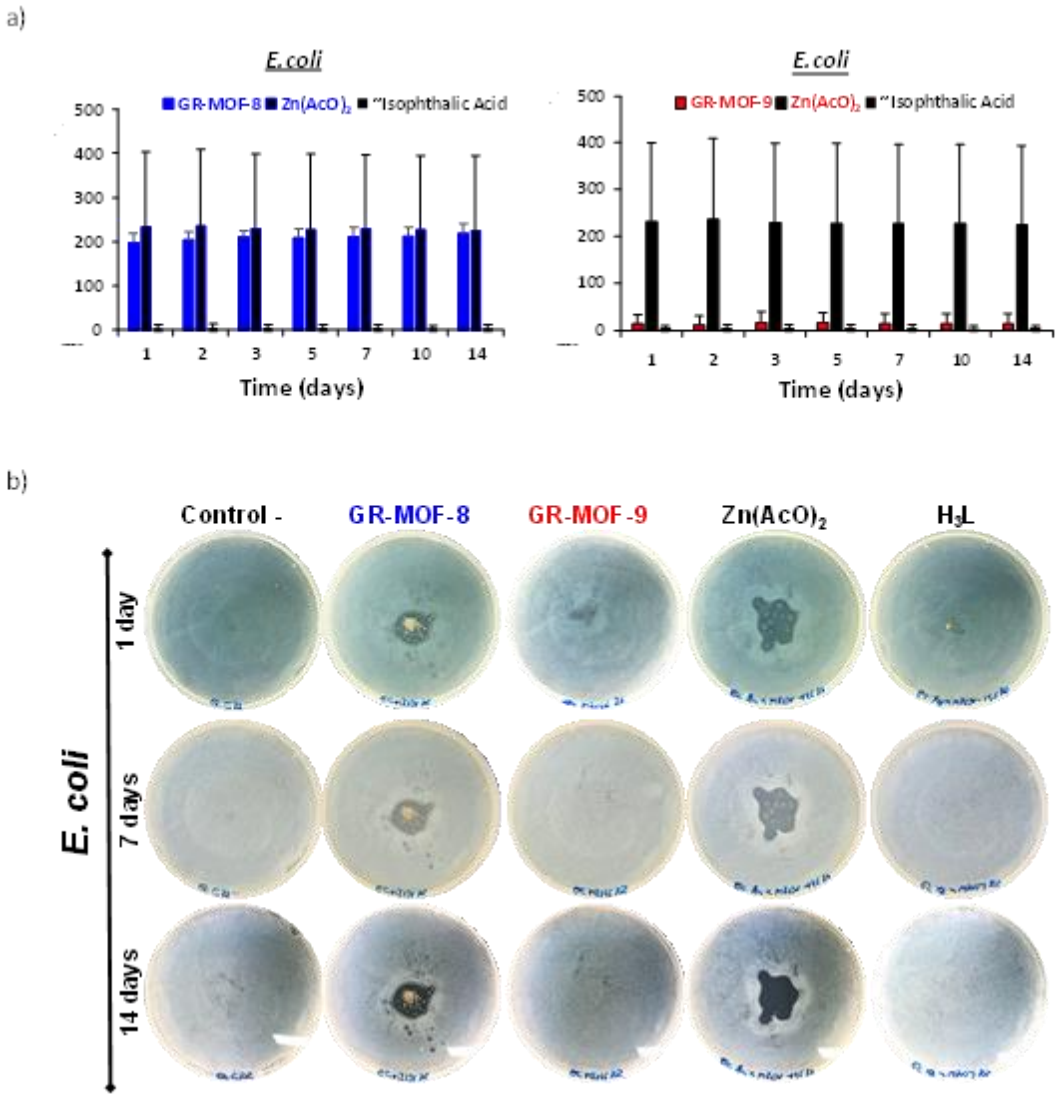


**Figure S6. a**) Halo inhibition zone experiments ($mm^2$) of GR-MOF-8 (blue), GR-MOF-9 (red) and their precursors: $Zn(AcO)_2 \cdot H_2O$, $H_3L$ and negative control (C-) after 14 days in contact with *E. coli* cultures in agar plates at 37 °C; **b**) Representative images of inhibition experiments with culture of *E. coli* corresponding to GR-MOF-8 and GR-MOF-9, $Zn(AcO)_2 \cdot H_2O$, $H_3L$ and negative control in the same conditions.

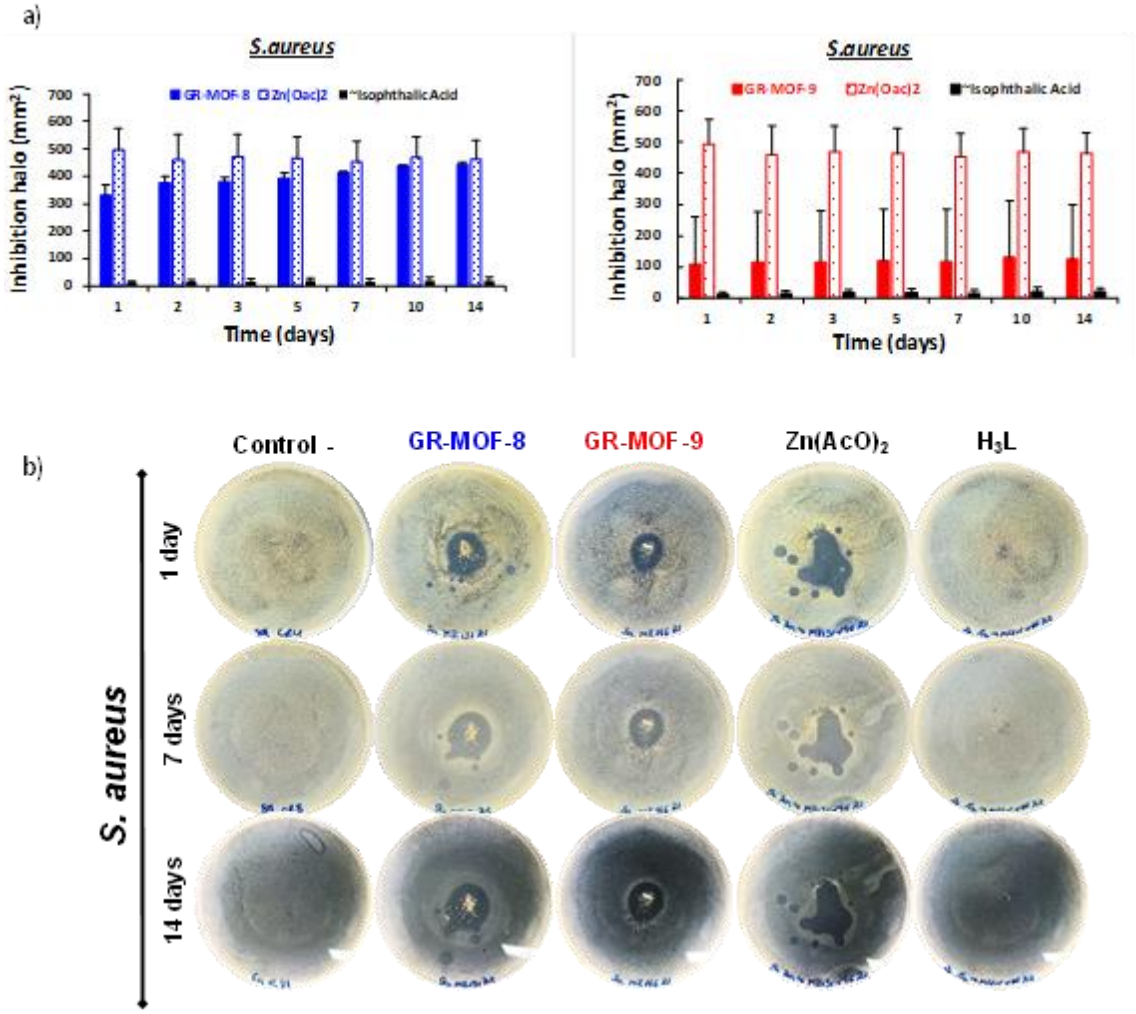


**Figure S7.** a) Halo inhibition zone experiments ($mm^2$) of GR.MOF-8 (blue), GR-MOF-9 (red) and their precursors: $Zn(AcO)_2{\cdot}H_2O$, $H_3L$ and negative control (C-) after 14 days in contact with *S. aureus* cultures in agar plates at 37 °C; b) Representative images of inhibition experiments with culture of *S. aureus* corresponding to GR-MOF-8 and GR-MOF-9, $Zn(AcO)_2{\cdot}H_2O$, $H_3L$, and negative control in the same conditions.

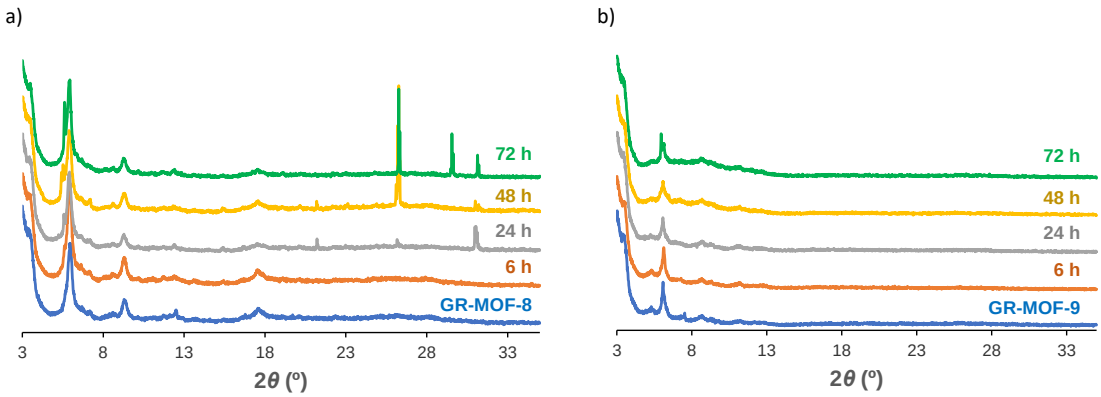


**Figure S8.** XRP diffraction stability studies of a) GR-MOF-8 and b) GR_MOF-9 in a high relative humidity (70%) ambient.